Molecular Geometry Inspired Positioning for Aerial Networks

Mustafa İlhan Akbaş, Gürkan Solmaz and Damla Turgut
Department of Electrical Engineering and Computer Science
University of Central Florida
Email: {miakbas,gsolmaz,turgut}@eecs.ucf.edu

***Abstract*— The advances in unmanned aerial vehicle (UAV) and wireless sensor technology made it possible to deploy aerial networks and to collect information in three dimensional (3D) space. These aerial networks enable high quality observation of events as multiple UAVs coordinate and communicate for data collection. The positioning of UAVs in aerial networks is critical for effective coverage of the environment and data collection. UAV systems have their characteristic constraints for node positioning such as dynamic topology changes or heterogeneous network structure. The positioning methods for two dimensional (2D) scenarios cannot be used for aerial networks since these approaches become NP-hard in 3D space.**

In this paper, we propose a node positioning strategy for UAV networks. We propose a wireless sensor and actor network structure according to different capabilities of the nodes in the network. The positioning algorithm utilizes the Valence Shell Electron Pair Repulsion (VSEPR) theory of chemistry, which is based on the correlation between molecular geometry and the number of atoms in a molecule. By using the rules of VSEPR theory, the actor nodes in the proposed approach use a lightweight and distributed algorithm to form a self organizing network around a central UAV, which has the role of the sink. The limitations of the basic VSEPR theory are eliminated by extending the approach for multiple central data collectors. The simulation results demonstrate that the proposed system provides high connectivity and coverage for the aerial sensor and actor network.

I. Introduction

The advances in unmanned aerial vehicle (UAV) systems made it possible to use autonomous or remotely operated UAVs in various applications such as environmental monitoring and battlefield surveillance. UAV solutions are cost effective and flexible compared to traditional aerial applications with personnel. The range of UAV applications has been increasing as UAVs have been equipped with multiple sensors for collecting different types of data such as thermal, visual or chemical observations. Although current approaches mostly use UAVs in solo flight, there are emerging concepts for employing multi-UAV systems as flying ad hoc networks (FANETs) [1]. Compared to a single UAV application, FANETs have several advantages such as scalability and survivability.

In a coordinated FANET, the capabilities and sizes of UAVs change according to their communication types to form a wireless sensor and actor network (WSAN) [2]. UAVs acting as sensor nodes are generally smaller and they only collect data from the environment. These small UAVs cannot carry heavy long distance communication hardware due to their limited weights and they are inexpensive compared to fully equipped research aircrafts, which act as actor nodes. Actor or sink UAVs require stronger communication hardware to communicate with an infrastructure or to communicate through longer distances. In addition to data collection, actor nodes also act on the environment by using actuators such as servo-mechanisms. For instance, low-flying helicopter platform by Thrun et al. [3] provides ground mapping and air-to-ground cooperation of autonomous robotic vehicles. Besides acting on the environment and collecting data, actor nodes perform networking functionalities such as processing or relaying of data in multi-UAV solutions. Therefore, these aerial networks are heterogeneous in terms of UAV types.

The application areas of FANETs expand continuously as the UAV technology is improved. We focus on application scenarios, in which the FANETs are used to cover the three dimensional (3D) space to execute the tasks of the system such as observation, monitoring or measurement. Volcanic plume sampling is one of these applications, where coordinated teams of UAVs are used to sample the airspace and provide an accurate mapping of distributed particles from recent volcanic eruptions [4]. These applications are time-critical since the maximum volume of the 3D space, where the plume is observed, must be covered and reported by the FANET. The efficient coverage of 3D space also plays an important role in atmospheric measurements. The Atmospheric Radiation Measurement (ARM) program [5] used UAV measurements to understand cloud and radiative processes. The FANETs provide expanded access to the atmosphere and clouds beyond what piloted aerial vehicles allow [6]. Therefore, FANETs allow studying 3D space for applications that are impossible with conventional aerial vehicles. In most of these applications, UAVs are deployed in regular topologies as they are deployed in an unrestricted aerial space and the main goal is the optimal coverage of 3D volume. However, they can also be integrated with obstacle avoidance approaches [7] for the cases where the UAV deployment is required to follow contours of the monitored area.

In this paper, an actor positioning strategy for aerial WSANs is presented to achieve 3D coverage while preserving 1-hop connectivity from each actor UAV to the central UAV in unprecedented settings of the scenario. The actors use a lightweight and distributed algorithm based on the Valence Shell Electron Pair Repulsion (VSEPR) theory [8] to form a

self organizing actor network. VSEPR theory is originally used in chemistry for the prediction of peripheral atom alignments around a central atom. This concept is adopted to define the rules of the algorithm designed to determine the actor positions. The basic VSEPR theory has limitations on the number of central and surrounding nodes. These limitations are eliminated by extending the adopted theory for multiple sinks to improve the scalability of the approach.

The main contributions of this paper are twofold. First, VSEPR theory is applied to the actor positioning based on the correlation between the molecular geometry and the number of atoms in a molecule. The approach creates a mapping between the actors and the electron pairs. Then the locations of actors are formulized according to the location of the sink and the properties of the VSEPR theory geometries. This positioning strategy is also extended for geometries up to 50% more actors. Second, an approach for the definition of multiple sink topologies is presented. For multiple sink scenarios, the capabilities of sink nodes are used to form a mesh network and to avoid a central coordinator node. The actors are shared by the sinks either in a balanced fashion or by using a preferential attachment based approach.

The rest of the paper is organized as follows. Section II summarizes the related work. We provide a detailed description for our approach in Section III. We present the simulation results in Section IV and finally conclude in Section V.

II. Related Work

Although there is an increasing interest in applications of sensor networks in 3D space such as space exploration or airborne surveillance, most of the literature on dynamic node positioning and routing strategies is limited to two dimensional (2D) space (see [9], [10], [11]). In the conventional 2D scenarios, the maximal coverage problem is mapped to a circle packing formulation which has a polynomial time solution. This problem turns into the sphere packing problem in three dimensions and the strategies designed for two dimensions become NP-hard in 3D space. The optimization strategies for 3D setups mostly focus on coverage problems.

Most of the 3D applications include assumptions such as homogenous node types or a priori knowledge of every location in the network for node positioning. These assumptions are not applicable in real life environmental monitoring scenarios, which have two important challenges. First, the problem of coverage in 3D space is a critical part of the scenario for the observation of an environment. The number of nodes and their locations are restricted by the investigated environment and the reception ranges of nodes. Second, the dynamic UAV network topology and flight must be handled efficiently considering the communication constraints of the vehicles. Ravelomanana [12] studies the properties of network topologies that result from random deployment of nodes in a 3D region of interest to provide the theoretical bounds. The study derives conditions for the node transmission range r required for achieving a degree of connectivity d, where every node has at least d neighbors. Li et al. [13] obtained the lower and upper bounds for capacities of both 3D regular and heterogeneous ad hoc networks. Akkaya and Newell [14] proposed a distributed node deployment scheme for underwater acoustic sensor networks. The nodes in this approach are relocated at different depths based on a local agreement in order to reduce the sensing overlaps among the neighboring nodes. Peppas and Turgut [15] has developed a hybrid routing algorithm for a specialized scenario consisting of a network of flying UAVs executing reconnaissance missions. Three different types of UAVs with various speeds, altitudes, and paths are considered for coordination of terrain identification process. Alam and Haas [16] argue that space filling polyhedrons would be more suitable for 3D coverage and aim to fill the 3D application space with the least number of polyhedrons for maximal coverage. Zhou et al. [17] present two algorithms for discovering boundary nodes and constructing boundary surfaces in 3D wireless networks. Bai et al. [18] designed and proved the optimality of one and two connectivity patterns under any value of the ratio of communication range over sensing range, among regular lattice deployment patterns. Slab Routing by Chiang and Peng [19] adapts 2D geographic face routing techniques to 3D space by dynamically creating a space partition and executing face routing over the planar projected graph of nodes contained within.

In our application scenario, UAVs have different properties depending on their functionalities. UAVs have been employed in a diverse set of fields including military [20] and science [21] applications as well as disaster monitoring [22]. The UAV industry have been doubled in the last decade according to market studies. Furthermore, there are companies and corporations providing custom-made vehicles with various capabilities. In the study of autopilot systems for small UAVs by Chao et al. [23], small-sized UAVs are defined to be lightweight with shorter wingspans and they are also cheap and expendable, which makes their development and operation easier compared to larger UAVs. Dempsey [24] grouped unmanned aircraft systems (UAS) into five categories according to their capabilities, advantages, and limitations. Group one UAS are typically hand-launched small vehicles capable of flying in altitudes less than 1200 feet above the ground level, whereas Group five UAS are the largest systems with extended capabilities in terms of endurance, air speed, range, and altitude. Table I presents a list of UAVs to exhibit their characteristics in terms of endurance, weight, and altitude.

The approach proposed in this paper can be integrated with different antenna solutions. The physical layer solution to be used in the application can be chosen according to the UAV properties and the mobile channel constraints, which would affect the range of nodes in the network. For instance, there are FANET applications using directional antenna for the communication reliability [26]. The localization approach by Jiang et al. [27] uses beacon nodes with rotating antennas to evaluate the received signal strength indication (RSSI) and arranges antenna orientations accordingly. Adaptive Medium Access Control protocol for UAV [28] is designed for FANETs with UAVs having both directional and omnidirectional antennas. In these FANETS, the UAVs have two directional antennas for data transmission and two omnidirectional antennas for localization. Temel and Bekmezci [29] use directional anten-

TABLE I: UAV Characteristics [25]

Vehicle	Endurance (h)	Payload weight (kg)	Maximum altitude (ft)
Aerosonde	40	1	20,000
Altus2	24	150	65,000
AV Black Widow	0.5	0.0	1,000
AV Dragoneye	1	0.5	3,000
AV Pointer	1.5	0.9	3,000
AV Puma	4	0.9	3,000
AV Raven	1.25	0.2	3,000
BQM-34	1.25	214	60,000
Chiron	8	318	19,000
Darkstar	8	455	45,000
Exdrone	2.5	11	10,000
Global Hawk	42	891	65,000
Gnat 750	48	64	25,000
MLB Bat	6	1.8	9,000
MLB Volcano	10	9	9,000
Pathfinder	16	40	70,000
Pioneer	5.5	34	12,000
Predator	29	318	40,000
Shadow 200	4	23	15,000
Shadow 600	14	45	17,000

nas with the location estimation of neighboring nodes to create a MAC layer protocol for FANETs. Zhang [30] compares the time delay in all-directional neighbor discovery for directional and omnidirectional antennas. The transmission range of the omnidirectional antennas limits their transmission capabilities. When using omnidirectional antennas, the transmitted data has a higher probability of packet loss compared to directional antennas. However, the complexity of the algorithm and the power requirements increase as the number of antennas increases.

There are aerial vehicle implementations for various applications concerning the aerial monitoring. The autonomous aerial system by Astuti et al. [4] has a single UAV, which performs aerial surveillance of volcanic areas and analysis of the composition of gases inside volcanic plumes. The SensorFly system [31] by Purohit and Zhang is a mobile-controlled flying sensor network designed to monitor changes in dangerous environments such as an earthquake or fire. SensorFly uses a flying miniature sensor with a weight of 30g and low mass production cost around $100. Elston and Frew [32] present a hierarchical control architecture with a mother-ship, a distributed database, and daughter micro air vehicles, which use vector field tracking. Autonomous flying robot multipurpose aerial robot vehicles with intelligent navigation (MARVIN) project [33] uses aerial robots with the ability to coordinate with each other to complete required tasks. SensorFlock by Allred et al. [34] is an airborne WSN composed of bird-sized micro aerial vehicles (MAVs), with a focus on the design of the MAVs and received signal strength indication (RSSI). The WSN of MAVs is composed of hundreds of inexpensive, semiautonomous, and cooperating airborne vehicles making observations and relaying data over a wireless communication mesh network. Luo et al. [35] propose a constant positioning and collision avoidance strategy for UAVs in outdoor search scenarios by using received signal strength (RSS) from the onboard communication module. Villas et al. [36] combine the tasks of localization in 3D and time synchronization by using a UAV equipped with a GPS flying over a sensor field. The sensor nodes in the field use the time and location information broadcasted by the UAV to estimate their locations and to synchronize.

Lee et al. [37] proposes a geometric deployment approach for addressing the deployment problem of an autonomous mobile robot swarm randomly distributed in 3D space. Each robot interacts with three neighboring robots in a selective and dynamic fashion without using any explicit communication so that four robots eventually form a regular tetrahedron. In our approach, we use VSEPR theory with geometric principles. VSEPR theory was first presented by Sidgwick and Powell [38] and refined by Gillespie and Nyholm [8]. VSEPR theory is based on the idea of a correlation between molecular geometry and the number of valence electrons around a central atom. According to VSEPR theory, the maximum repulsion of the electron pairs or atoms defines the optimum geometric positions of peripheral atoms or alone electron pairs that maximizes the distance between these entities. This characteristic of VSEPR theory is used in our approach to form the optimum geometries for 3D coverage.

III. Positioning model

The aerial network has a hierarchical structure of nodes in our application scenario. Small UAVs have built-in sensors and they have limited payload capacities. The hierarchical structure allows utilization of these small UAVs for complicated missions in larger volumes since these nodes are affiliated to a set of more powerful actor nodes. The sinks are the largest UAVs in the network with highest communication capabilities. This hierarchical structure requires coordination among nodes for successful operation and positioning is critical for an efficient coordination of UAVs in the network.

The nodes follow no predetermined initial configuration for the formation of actor-sink backbone and affiliation of sensor nodes with the actors. Each sensor node s communicates only with direct neighbors $Neigh(s)$ and keeps a "weight" value, which is "k-(hop distance)" where k is the weight of the actor and hop distance is the number of hops required to reach the

affiliated actor. The sensor nodes and actors are assumed to have transmission radii r_s and r_a, respectively, with spherical transmission ranges.

A. "VSEPR theory" approach

The VSEPR model is the most successful model for the prediction of closed-shell molecule geometries. Laplacian of the charge density provides the physical basis for the VSEPR model. Within a molecule, the Laplacian of the electronic charge density exhibits extrema in the valence shell of the central atom. These extrema indicate the presence of localized concentrations of electronic charge. The spherical surface on which the electron pairs are assumed to be localized is identified with the sphere of maximum charge concentration in the valence-shell charge concentration and the localized pairs of electrons are identified with the local maxima.

VSEPR theory uses the "AXE method" of electron counting, in which A is the number of central atoms, X is the number of sigma bonds between the central atom and the surrounding atoms and E is the number of lone electron pairs. The geometry predictions depend on the steric number, which is the sum of X and E. E is used particularly for deciding the positions of the actors in systems with multiple sinks in our approach.

We form an analogy between the VSEPR theory and the positioning of actors around the sink. According to this analogy, the possible positions of actors are found by using VSEPR theory geometries. The VSEPR theory geometry to be used in the system depends on the number of actors in the network. It's stated in VSEPR theory that the electron pairs surrounding the central atom repel each other. This repulsion is minimized when the orbitals containing electron pairs point as far away from each other as possible. To find the repulsion forces among electron pairs, Gillespie [39] assumes the electron pairs are located on impenetrable orbitals.

In the real molecular structure, there are interpenetrations or overlaps in the electron orbitals, which makes it impossible to define a constant force between two electron pairs. However, the favored arrangement of the electron pairs in a molecule is shown to be independent of the changing characteristics of the forces among electron pairs except for the case of seven pairs. Therefore, the favored arrangements of VSEPR theory are identified according to the impenetrable orbital approach. With this assumption, the least distance between any two pairs of electrons is maximized as they repel each other and the geometries are identified as given in Fig. 1.

In our approach, each geometry around the sink corresponds to the polyhedron whose number of vertices is equal to the number of surrounding actors. For the exceptional case of seven nodes, there are two possible arrangements, the monocapped trigonal prism and the pentagonal bipyramid. We use the latter in our scenarios as demonstrated in Fig. 1.

All of the geometries are formulated such that the actor positions are defined with respect to the position of the sink. The algorithm provides self organization of the system for increasing and decreasing number of actors.

B. VSEPR theory geometries of WSAN and positioning

The position of the sink, (x_s, y_s, z_s), is taken as the reference origin in XYZ coordinate system during the flight and all other positions are calculated with respect to this origin. The formulation of geometries is critical for the definition of positions that the actors can be located and for the definition of transitions between geometries. The main direction that the UAV system headed on a time instant forms the x-coordinate and the positions of the actors are formulated according to this system.

The radius of a geometry is defined as the distance between an actor node and the sink in that geometry and the radius of each geometry is r_a when the actors are not required to communicate with neighbors and communicate only with the sink node. However, the distances among the actors are different for each geometry and the radius of a geometry such that each node can communicate at least with one neighbor or with all other actors depends on the positions of the actors in that geometry. Therefore, we define the distances among actors in terms of r_a for each geometry and give an equation to determine the radius of each geometry.

When there are two actors, they are arranged in a "Linear" geometry, with an expected connection angle of 180° and following positions:

$$p_{a_1}(x,y,z)=(x_s+r, y_s, z_s)$$
$$p_{a_2}(x,y,z)=(x_s-r, y_s, z_s)$$

The radius of the linear geometry becomes $\frac{r_a}{2}$ when a direct communication between two actors is required since the distance from the sink to each actor decreases from r_a to $\frac{r_a}{2}$.

The geometrical model used when there are three actors around the sink is "Trigonal planar". According to VSEPR theory, the repulsion between three atoms will be at a minimum when the angle between any two is $(360^\circ \div 3) = 120^\circ$. In this geometry, all actors and the sink are in the same plane and the actors are in the following positions:

$$p_{a_1}(x,y,z)=(x_s+r, y_s, z_s)$$
$$p_{a_2}(x,y,z)=(x_s-r\cdot sin(30^\circ), y_s+r\cdot sin(60^\circ), z_s)$$
$$p_{a_3}(x,y,z)=(x_s-r\cdot sin(30^\circ), y_s-r\cdot sin(60^\circ), z_s)$$

In "Trigonal planar" geometry, the distance between any two actors is $R\sqrt{3}$, where R is the distance of an actor node from the sink. Therefore, actors can communicate only with the sink in the original positioning scenario, where R is r_a. The radius of this geometry such that each node can communicate at least with its neighbors is $\frac{r_a\sqrt{3}}{3}$.

When there are four peripheral actor UAVs, four equivalent bonds point in four geometrically equivalent directions in three dimensions corresponding to the four corners of a tetrahedron centered on the sink. The angle between any two connections is $cos^{-1}(\frac{-1}{3}) \approx 109.5^\circ$. Therefore, the actors are positioned in following locations:

$$p_{a_1}(x,y,z)=(x_s, y_s, z_s+r)$$
$$p_{a_2}(x,y,z)=(x_s-r\cdot a, y_s-r\cdot b, z_s+r\cdot cos(109.5^\circ))$$
$$p_{a_3}(x,y,z)=(x_s-r\cdot sin(109.5^\circ), y_s, z_s+r\cdot cos(109.5^\circ))$$
$$p_{a_4}(x,y,z)=(x_s-r\cdot a, y_s+r\cdot b, z_s+r\cdot cos(109.5^\circ))$$

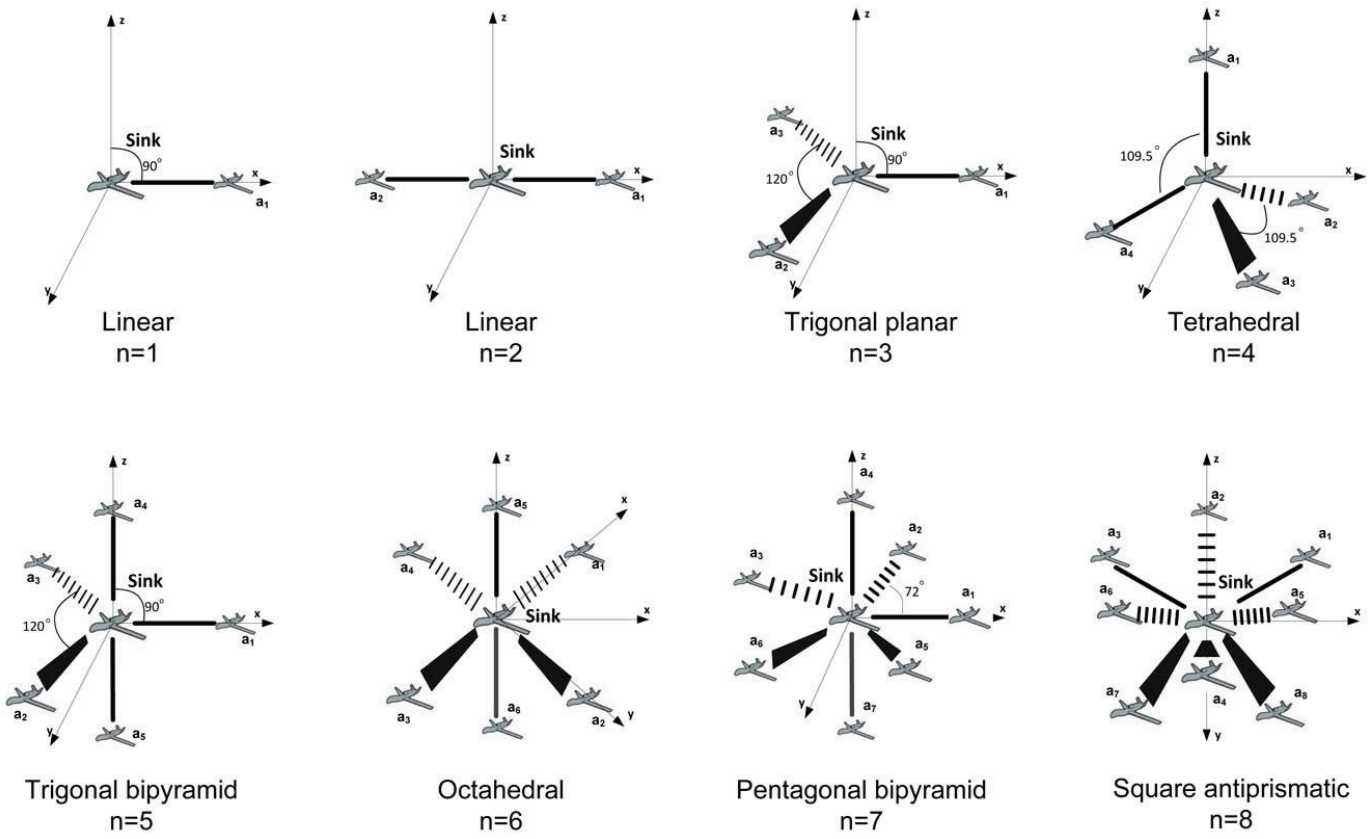

Fig. 1: VSEPR theory geometries.

where $a = sin(109.5°) \cdot sin(30°)$, $b = sin(109.5°) \cdot cos(30°)$.

In the geometry with four actors, the distance between any two actors is $R\frac{4}{\sqrt{6}}$, where R is the distance of an actor node from the sink. The radius of this geometry such that each node can communicate at least with its neighbors is $\frac{r_a\sqrt{6}}{4}$.

In the cases of two, three, four, and six actors, actors are distributed as far apart as possible on the surface of a sphere. For four and six actors, the resulting shapes correspond to the regular polyhedron having the same number of sides. There is no regular polyhedron with five vertices when the number of actors become five.

When there are five actors, they take positions with non-identical connection angles. Three actors are positioned on the $y = 0$ plane with connection angles of $120°$ whereas the other two actors take positions on y-axis with angles of $90°$ to the $y = 0$ plane. Hence this geometry is a Trigonal bipyramid. This geometry consists of two triangular-base pyramids joined base-to-base and the actors are positioned in following locations:

$$
\begin{aligned}
&p_{a_1}(x,y,z)=(r + x_s, y_s, z_s)\\
&p_{a_2}(x,y,z)=(x_s - r \cdot sin(30°), y_s + r \cdot sin(60°), z_s)\\
&p_{a_3}(x,y,z)=(x_s - r \cdot sin(30°), y_s - r \cdot sin(60°), z_s)\\
&p_{a_4}(x,y,z)=(x_s, y_s, r + z_s)\\
&p_{a_5}(x,y,z)=(x_s, y_s, z_s - r)
\end{aligned}
$$

Since the actors take positions with non-identical connection angles in five-actor geometry, the distances among the actors also differ according to their positions and take values $R\sqrt{3}$, $R\sqrt{2}$ and $2R$, where R is the distance from the sink to an actor.

There are two important values of the radius for five-actor geometry. The radius of this geometry such that each node can communicate with all other actors is $\frac{r_a}{2}$. The radius of the geometry such that each node can communicate with at least one neighbor is $\frac{r_a\sqrt{3}}{3}$.

When there are six actors, they are arranged around the sink symmetrically, defining the vertices of an octahedron. An octahedron is composed of two square-based pyramids joined base-to-base and it has three equivalent four-fold symmetry axes, resulting in the following actor positions:

$$
\begin{aligned}
&p_{a_1}(x,y,z)=(x_s + r, y_s, z_s)\\
&p_{a_2}(x,y,z)=(x_s, y_s + r, z_s)\\
&p_{a_3}(x,y,z)=(x_s - r, y_s, z_s)\\
&p_{a_4}(x,y,z)=(x_s, y_s - r, z_s)\\
&p_{a_5}(x,y,z)=(x_s, y_s, z_s + r)\\
&p_{a_6}(x,y,z)=(x_s, y_s, z_s - r)
\end{aligned}
$$

The radius of the six-actor geometry is $\frac{r_a}{2}$ for each node to communicate with all other actors. The radius of the geometry such that each node can communicate with at least one neighbor is $\frac{r_a\sqrt{2}}{2}$.

The pentagonal bipyramid (or dipyramid) is a molecular geometry with one atom at the center with seven ligands at

the corners of a pentagonal dipyramid.

$$p_{a_1}(x,y,z)=(x_s+r, y_s, z_s)$$
$$p_{a_2}(x,y,z)=(x_s+r\cdot cos72°, y_s+r\cdot sin72°, z_s)$$
$$p_{a_3}(x,y,z)=(x_s-r\cdot cos36°, y_s+r\cdot sin36°, z_s)$$
$$p_{a_4}(x,y,z)=(x_s, y_s, z_s+r)$$
$$p_{a_5}(x,y,z)=(x_s+r\cdot cos72°, y_s-r\cdot sin72°, z_s)$$
$$p_{a_6}(x,y,z)=(x_s-r\cdot cos36°, y_s-r\cdot sin36°, z_s)$$
$$p_{a_7}(x,y,z)=(x_s, y_s, z_s-r)$$

Similar to the six-actor geometry, the radius is $\frac{r_a}{2}$ for each node to communicate with all other actors in the pentagonal dipyramid geometry. The radius of the geometry such that each node can communicate with at least one neighbor is $\frac{r_a\sqrt{2}}{2}$.

According to the VSEPR theory, the square antiprism is the favored geometry among the possible geometries with eight surrounding atoms. A square anti-prism corresponds to the shape when eight points are distributed on the surface of a sphere as follows:

$$p_{a_1}(x,y,z)=(x_s+r\cdot a\tfrac{\sqrt{2}}{2}, y_s, z_s+r\cdot\tfrac{h}{2})$$
$$p_{a_2}(x,y,z)=(x_s, y_s+r\cdot a\tfrac{\sqrt{2}}{2}, z_s+r\cdot\tfrac{h}{2})$$
$$p_{a_3}(x,y,z)=(x_s-r\cdot a\tfrac{\sqrt{2}}{2}, y_s, z_s+r\cdot\tfrac{h}{2})$$
$$p_{a_4}(x,y,z)=(x_s, y_s-r\cdot a\tfrac{\sqrt{2}}{2}, z_s+r\cdot\tfrac{h}{2})$$
$$p_{a_5}(x,y,z)=(x_s+r\cdot a, y_s+r\cdot a, z_s-r\cdot\tfrac{h}{2})$$
$$p_{a_6}(x,y,z)=(x_s-r\cdot a, y_s+r\cdot a, z_s-r\cdot\tfrac{h}{2})$$
$$p_{a_7}(x,y,z)=(x_s-r\cdot a, y_s-r\cdot a, z_s-r\cdot\tfrac{h}{2})$$
$$p_{a_8}(x,y,z)=(x_s+r\cdot a, y_s-r\cdot a, z_s-r\cdot\tfrac{h}{2})$$

where a and h are constants used in square antiprism geometry to simplify the transitions. $h/2 \approx 0.5237$ represents the positive and negative z values for the planes that the actors are located at and $a \approx 1.2156$. Using these values, we also find the radius of the geometry for each node to communicate with all other actors, which is $r_a 0.235(2\sqrt{2}-1)$.

Our dynamic application scenario includes various requirements and challenges because of its differentiating features such as the lack of human control or the continuous motion during the flight. Therefore the geometries must not be very sensitive to small changes in positions and the actors must be able to reorganize in case of a change in the number of actors. Algorithm 1 presents our positioning strategy for actors around a central sink node at (x_s, y_s, z_s).

In Algorithm 1, the common properties of calculated positions of actors in the specific geometries are used. All actor positions defined according to Algorithm 1 are on $z = z_s$ plane when n is smaller than four with the condition $\Theta = \frac{360}{n}$. When n is equal to four, the geometry is perfectly symmetrical. Therefore, the actor closest to $z = r$ plane takes (x_s, y_s, r) position and all the other nodes are located with equal distances to each other. When n is between four and eight, there are two actors on z axis and the others are on $z = 0$ axis plane. When the number of actors is larger than seven, the actors are positioned at least on two planes instead of one with a certain z value.

Algorithm 1 Actor positioning

r: Distance from an actor to the sink
$\vec{p}$: Position vector of a node
Θ: Angle between $\vec{p}_s$ and $\vec{p}_i$
(x_s, y_s, z_s): Coordinates of the sink
if $n < 4$ **then**
  All actors are position at $z = z_s$ plane with $\Theta = \frac{360}{n}$
  One actor is positioned at $(x_s + r, y_s, z_s)$
  $i = \Theta$
  while $i < 360°$ **do**
    Next actor is positioned at $(x_s + r \cdot cos(\Theta), y_s, z_s)$
    $i = i + \Theta$
  end while
else if $n = 4$ **then**
  $\Phi = -19.471°$
  One actor is positioned at $(x_s, y_s, z_s + r)$
  $i = 0°$
  while $i < 360°$ **do**
    Next actor is positioned at (x_a, y_a, z_a)
    $x_a = r \cdot cos(i) \cdot cos(\Phi) + x_s$
    $y_a = r \cdot sin(i) \cdot cos(\Phi) + y_s$
    $z_a = r \cdot sin(\Phi) + z_s$
    $i = i + 120°$
  end while
else if $8 > n > 4$ **then**
  Two actors are positioned on (x_s, y_s) line
  One of remaining actors is positioned at $(x_s + r, y_s, z_s)$
  $\Theta = \frac{360}{n-2}$ on $z = 0$ plane
  $i = \Theta$
  while $i < 360°$ **do**
    Next actor is positioned at $(x_s + r \cdot cos(i), y_s + r \cdot sini, z_s)$
    $i = i + \Theta$
  end while
else if $n = 8$ **then**
  $\frac{h}{2} = 0.5237$, $a = 1.2156$:
  Positions:
  $x_s \pm r \cdot a, y_s \pm r \cdot a, z_s - r \cdot \frac{h}{2}$ for first four actors
  $x_s \pm r \cdot \frac{a}{\sqrt{2}}, y_s, z_s + r \cdot \frac{h}{2}$ for two actors
  $x_s, y_s \pm r \cdot \frac{a}{\sqrt{2}}, z_s + r \cdot \frac{h}{2}$ for remaining actors
end if

C. Extension of VSEPR theory approach

We extended our initial approach by using an approach from molecular geometry. The compounds in nature have less than eight peripheral atoms. Therefore the initial VSEPR theory was presented for one central atom and at most eight surrounding atoms. Most of the current applications of UAV systems are composed of less number of actor UAVs [1]. Therefore, APAWSAN [40] employed only the basic VSEPR theory for actor positioning. Adoption of this theory allowed the design of a system with at most eight actor UAVs and larger number of small UAVs. However the number of nodes in the network and the total covered volume can be increased if this approach is improved by including more actor nodes. The approach for the determination of actor positions is improved. We use the position of the sink at any time instant for the extension and give two different algorithms for basic and extended geometries. The extended geometries are for up to

50% more actors depending on the repulsion force rules in molecular geometry.

Gillespie [39] applied the rules of VSEPR theory for up to twelve actors and presented an application of the theory for these higher number of surrounding nodes around a central node. These geometries are formed depending on the same repulsion force rules used in initial VSEPR theory. Hence we extended our approach by utilizing VSEPR theory principles to allow deployment of more than eight actors.

The geometries for nine to twelve actors, shown in Fig. 2, are monocapped square antiprism, bicapped square antiprism, icosahedron minus one apex and icosahedron. The monocapped square antiprism in our approach corresponds to the geometry with the one more actor location $p_{a_9}(x,y,z) = (x_s, y_s, z_s + r)$ additional to square antiprism. For bicapped square antiprism, there is one more actor positioned at $p_{a_{10}}(x,y,z) = (x_s, y_s, z_s - r)$.

The icosahedron is a geometrical shape composed of twenty triangular faces, thirty edges and twelve vertices. Icosahedron minus one apex is an icosahedron with one missing vertex. The favored geometry for twelve actor geometry is a regular icosahedron with identical equilateral faces and the following actor positions:

$$
\begin{aligned}
&p_{a_1}(x,y,z)=(x_s, y_s + \tfrac{r}{2}, z_s + r \cdot \tfrac{\sqrt{5}-1}{4})\\
&p_{a_2}(x,y,z)=(x_s, y_s - \tfrac{r}{2}, z_s + r \cdot \tfrac{\sqrt{5}-1}{4})\\
&p_{a_3}(x,y,z)=(x_s, y_s + \tfrac{r}{2}, z_s + -r \cdot \tfrac{\sqrt{5}-1}{4})\\
&p_{a_4}(x,y,z)=(x_s, y_s - \tfrac{r}{2}, z_s - r \cdot \tfrac{\sqrt{5}-1}{4})\\
&p_{a_5}(x,y,z)=(x_s + \tfrac{r}{2}, y_s + r \cdot \tfrac{\sqrt{5}-1}{4}, z_s)\\
&p_{a_6}(x,y,z)=(x_s - \tfrac{r}{2}, y_s + r \cdot \tfrac{\sqrt{5}-1}{4}, z_s)\\
&p_{a_7}(x,y,z)=(x_s + \tfrac{r}{2}, y_s - r \cdot \tfrac{\sqrt{5}-1}{4}, z_s)\\
&p_{a_8}(x,y,z)=(x_s - \tfrac{r}{2}, y_s - r \cdot \tfrac{\sqrt{5}-1}{4}, z_s)\\
&p_{a_9}(x,y,z)=(x_s + r \cdot \tfrac{\sqrt{5}-1}{4}, y_s, z_s + \tfrac{r}{2})\\
&p_{a_{10}}(x,y,z)=(x_s - r \cdot \tfrac{\sqrt{5}-1}{4}, y_s, z_s + \tfrac{r}{2})\\
&p_{a_{11}}(x,y,z)=(x_s + r \cdot \tfrac{\sqrt{5}-1}{4}, y_s, z_s - \tfrac{r}{2})\\
&p_{a_{12}}(x,y,z)=(x_s - r \cdot \tfrac{\sqrt{5}-1}{4}, y_s, z_s - \tfrac{r}{2})
\end{aligned}
$$

The positioning algorithm for extended geometries is given in Algorithm 2. The similarities of the geometries are used to define the locations. According to the Algorithm 2, in geometries with even number of actors, two actors are positioned on (x_s, y_s) line with r distance from the sink. If the number of actors is odd, a single actor will be positioned on (x_s, y_s, z_s). The rest of the actors are positioned on two planes such as $z_s \pm h$, where h is calculated according to the geometry. On these planes, the actors are distributed with equal angles and two planes are positioned with an angle of $\frac{360}{n-2}$ and $\frac{360}{n-1}$ between them for even and odd number of actors respectively.

Kettle [41] showed that the usual molecular orbitals which are used to describe the bonding in the metal cluster may be transformed into the localized two-center and three-center molecular orbitals described by VSEPR theory. When there are more than twelve actors, our system requires multiple sinks to form the actor geometries. Therefore, the requirement of our approach is the deployment of more than one sink as the number of actors exceeds twelve.

Algorithm 2 Actor positioning for extended geometries

n: Number of actors
a_i: Actor i
if n is even **then**
  Two actors are positioned on $(x_s, y_s, z_s \pm r)$ line
else
  One actor is positioned on $(x_s, y_s, z_s + r)$
end if
if $n < 11$ **then**
  $\frac{h}{2} = 0.5237$, $a = 1.2156$:
  for $i = 1 \rightarrow 4$ **do**
    $x_s \pm r \cdot a, y_s \pm r \cdot a, z_s - r \cdot \frac{h}{2}$
  end for
  for $i = 5 \rightarrow 6$ **do**
    $x_s \pm r \cdot \frac{a}{\sqrt{2}}, y_s, z_s + r \cdot \frac{h}{2}$
  end for
  For remaining actors: $x_s, y_s \pm r \cdot \frac{a}{\sqrt{2}}, z_s + r \cdot \frac{h}{2}$
else
  $\Phi = 26.565$ and $\Theta = 0°$
  for $i = 1 \rightarrow 5$ **do**
    $x_a = r \cdot cos(\Theta) \cdot cos(\Phi)$, $y_a = r \cdot sin(\Theta) \cdot cos(\Phi)$, $z_a = r \cdot sin(\Phi)$
    $\Theta = \Theta + 72°$
  end for
  $\Theta = 36°$
  for $i = 6 \rightarrow 10$ **do**
    $x_a = r \cdot cos(\Theta) \cdot cos(-\Phi)$, $y_a = r \cdot sin(\Theta) \cdot cos(-\Phi)$, $z_a = r \cdot sin(-\Phi)$
    $\Theta = \Theta + 72°$
  end for
end if

D. Multiple sinks

The scalability of our approach is improved by using multiple sink nodes as another extension of VSEPR theory based method in our system. APAWSAN [40] uses basic VSEPR theory geometries and has no multiple sink scenarios. In this paper, an algorithm for the formation of sink network is proposed and the geometrical requirements introduced by the multiple sink geometries are calculated. In multiple sink geometries, we propose two strategies for the distribution of actors among sinks. The first strategy utilizes a preferential attachment based method. In the second proposed strategy, the actors are distributed among the sinks in a balanced fashion.

It has been shown in molecular geometry that the molecules containing multiple central atoms and bonds conform to the general rule of the repulsion among the electron pairs around any central atom. The multiple sink scenario of our approach is modeled as the case with multiple central atoms in the molecular geometries.

Utilization of multiple sinks extends the endurance and scalability of the operation of multiple UAV systems. Since the scenarios with a single sink node use VSEPR theory by forming an analogy to a molecule with a central atom, scenarios with multiple sinks utilize VSEPR theory with an analogy to the connection of multiple molecules. Sinks are larger UAVs

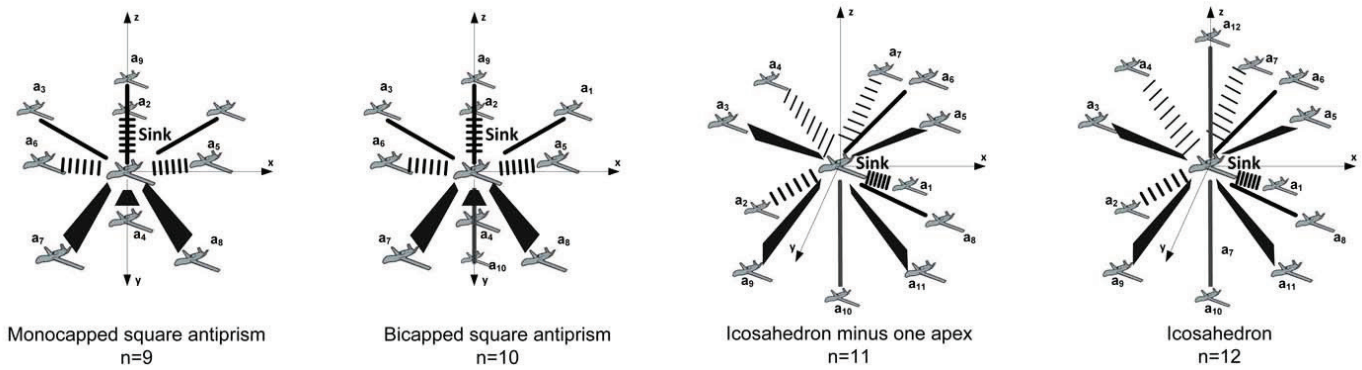

Fig. 2: VSEPR geometries for nine to twelve actors.

with higher payload capacities compared to actors and they are less prone to issues related to weight. While actors are capable of carrying relatively heavier communication hardware as a result of these properties, the lighter payload means the higher altitude and the longer endurance for smaller UAVs [42]. Therefore sinks are used in the aerial network to form the backbone, which is composed of longer communication links. The actors operate with lighter communication hardware by affiliating with a sink and positioning themselves according to VSEPR theory around the sink.

The network of sinks form one of the favored geometries of basic VSEPR theory. For instance, if there are six sinks in an aerial WSAN, they are positioned as the vertices of octahedral without a central node. An example of multiple sink geometries is given in Fig. 3. Four sinks form the tetrahedral geometry with an actor connected to each sink. The sinks are positioned according to the VSEPR theory rules such that each one forming tetrahedral geometries with three actors and a sink.

There are three main objectives for excluding the central node in the formation of the VSEPR geometries with sinks. First, the communication ranges of sink nodes are larger compared to the actor nodes. As a result, sinks can form a mesh network among themselves, covering an adequately large volume for the mission, without the requirement of a central node with stronger capabilities. Second, introduction of another node type would increase the complexity of the heterogeneous network. Third, the utilization of multiple sinks divides the role of the sink in multiple nodes and prevents the single point of failure. Systems with multiple UAVs operate in highly dynamic environments. The conditions at the beginning of a mission may change during the operation. Therefore the system's ability of adapting to changes in the number of sinks is an important advantage as the number of nodes in the system increases.

The positioning of sinks according to VSEPR theory rules is both challenging and different compared to actor positioning around a central sink. The sinks form a mesh network, which act as the core of the overall UAV system. The defined flight route determines the central point of the geometries and this is shared by all of the sinks. The distances between the sinks change according to the geometries. The edge distances for sink geometries are given in Table II. The transmission range of each sink must be larger than longest edge in the network for a mesh network of sinks.

The sinks form the network by sharing their information with each other. Each of the sinks transmits a network formation packet (NFP) with its ID in the source field and the number of actors connected to it in the payload. The processing of NFP at a sink a is given in Algorithm 3. The sinks record the IDs of the sinks, which they received NFP from, and they calculate the number of the sinks using this information. The sink list is used at a sink for positioning. This list is also saved and updated for future use in case of a change in the backbone network such as adding or removing a sink node. If an NFP is received from a sink, which has a number of actors less than the average, next NFP is loaded with a query for update to this sink. In this way, the sinks with less number of actors employ actors from other sinks. Essentially, our approach keeps a balanced backbone network in terms of the number of actors.

Algorithm 3 Processing of NFP message at sink a

n_s: Number of actors for a sink s
S: Sink list kept at the sink a
E: List for unbalanced sinks
Update S
for Each sink i in S **do**
  Update n_i
  if $n_i < \lfloor \frac{\sum_{i=1}^{n(S)} n_i}{n(S)} \rfloor$ **then**
    Add i in E
  else if $i \in E$ **then**
    Remove i from E
  end if
end for
if $n_a > \frac{\sum_{i=1}^{n_s} n_i}{n_s}$ **then**
  if $E \neq \emptyset$ **then**
    for Each sink $j \in S$ **do**
      Send NFP with query for update
    end for
  end if
end if

The first strategy for multiple sink geometries is the VSEPR theory based positioning with preferential attachment based

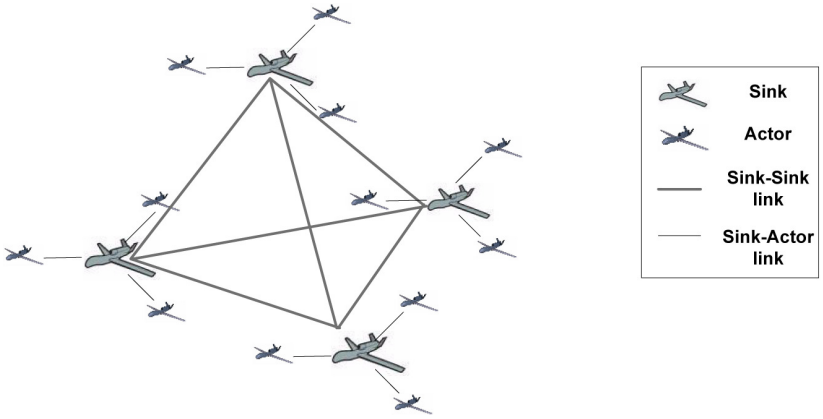

Fig. 3: An example of multiple sink geometries.

TABLE II: Distances between sinks for multiple sink networks

Geometry	**Sink edge distances**
Linear	R
Trigonal planar	$R\sqrt{3}$
Tetrahedron	$R\frac{4}{\sqrt{6}}$
Trigonal bipyramid	$R\sqrt{3}$, $R\sqrt{2}$, $2R$
Octahedron	$R\sqrt{2}$, $2R$
Pentagonal dipyramid	$R\sqrt{2}$, $2R$, $R\sqrt{(5-\sqrt{5})/2}$,$R\sqrt{(5+\sqrt{5})/2}$
Square antiprism	$R\frac{1}{1.645}(2+\frac{1}{\sqrt{2}})$, $R\frac{1}{1.645}(2+\frac{1}{\sqrt{2}})\sqrt{2}$, $R\frac{1}{1.645}\sqrt{1+\sqrt{3}+2\sqrt{2}}$

actor deployment (VTPA). There is no limitation in the node degree of existing preferential attachment models, which violates the requirement of upper limit on the number of actors for VSEPR theory approach. Therefore in VTPA, we define a cutoff preferential attachment model, which defines a "maximum degree" for the sink node based on our VSEPR theory approach. The actors are deployed according to the preferential attachment until one of the nodes has the "maximum degree". In this case, that sink becomes ineligible for new actors to get connected. The second strategy is VSEPR theory based positioning with balanced actor deployment (VTBP), by which the actors are distributed among the sinks in a balanced fashion. Therefore, if there is a new actor added to the network in this method, it is connected to the sink with the lowest number of actors.

IV. Simulation Study

The evaluation of the proposed system is conducted in OPNET modeler [43]. The node models are created in OPNET modeler with the default transmission radius of 40 meters and IEEE 802.11 MAC layer. The performance of the approach is evaluated for the coverage of the geometries, weight values of the nodes, cardinality of the actors and the network characteristics of the formed geometries.

A. Coverage

The first performance metric used for evaluation is the total coverage volume, which is the union of all actor coverages. The union volume of actor coverage is calculated by a numerical approach, which first finds the most distant point in the coordinate system. Then, the real coordinate system is projected to a boolean 3D matrix. The boundary points are found for each sphere and points fitting into the sphere are used to calculate the final volume.

When sensor nodes collect information from the environment, there must be at least one actor in a sensor node's transmission range, which makes the coverage of the network backbone critical for the performance of the system. The inputs for the volume calculation of actor coverage are the number of spherical coverage volumes, coordinates of the actors, the reception range and the expected memory usage by matrix used for modeling spheres. The union volume of actor coverage is calculated by using these inputs.

Fig. 4 shows coverage for geometries with one sink, two sinks and "3D Deployment" by Lee et al. [37]. Our approach outperforms "3D Deployment" with an average volume difference of 22%. As the number of actors increases up to nine, the coverage of the basic VSEPR theory geometries increase. However it can be observed that the bicapped square antiprism, icosahedron minus one apex and icosahedron are not as effective as the geometries with less actors. Additionally, it is observed that the coverage of 1-sink and 2-sink geometries are similar unless the number of data collectors exceeds seven. Therefore, the number of sinks must be increased to change the geometry of the actors for a more effective coverage when the number of actors exceeds seven.

In the second set of experiments, the coverage of the proposed VSEPR theory based positioning (VTBP) approach is compared to a partially random positioning (PRP) method. PRP method is designed such that it includes the same number of the sink nodes for each geometry to compare and each actor node is at the same distance to retain the properties of network

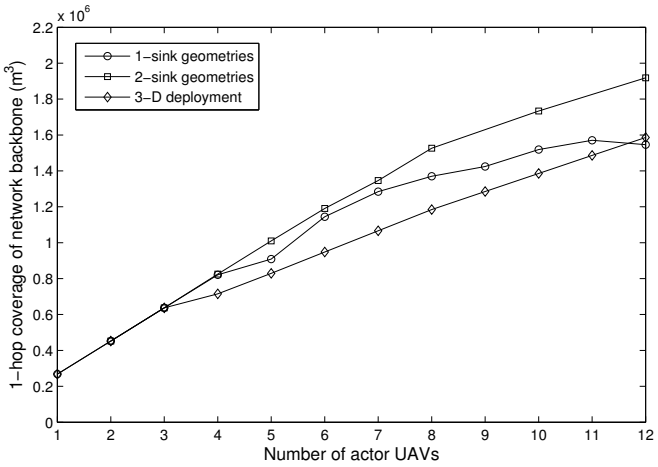

Fig. 4: 1-hop coverage for different geometries.

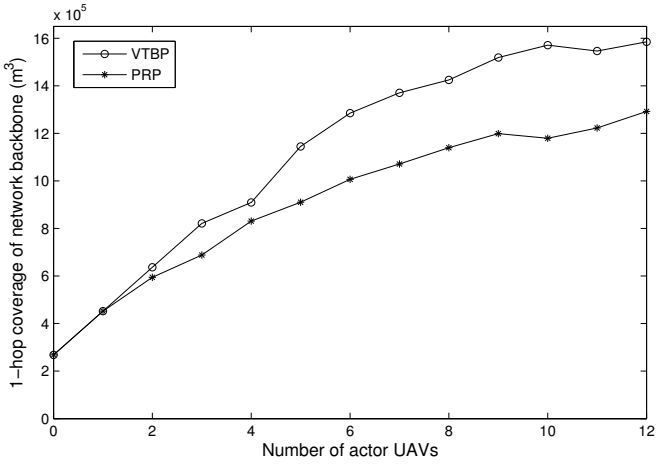

Fig. 5: 1-hop coverage for our protocol vs. random positioning with 1 sink.

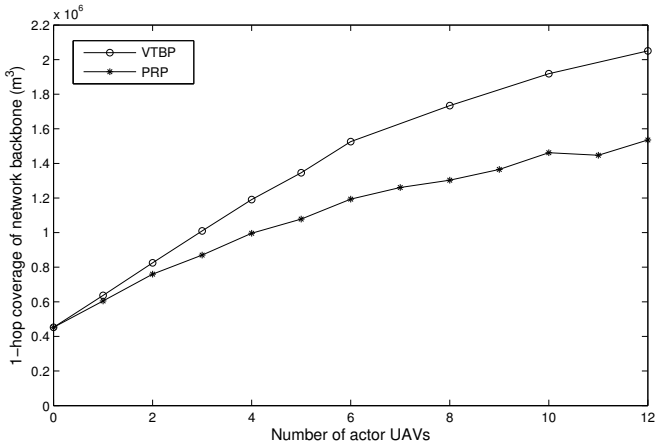

Fig. 6: 1-hop coverage for our protocol vs. random positioning with 2 sinks.

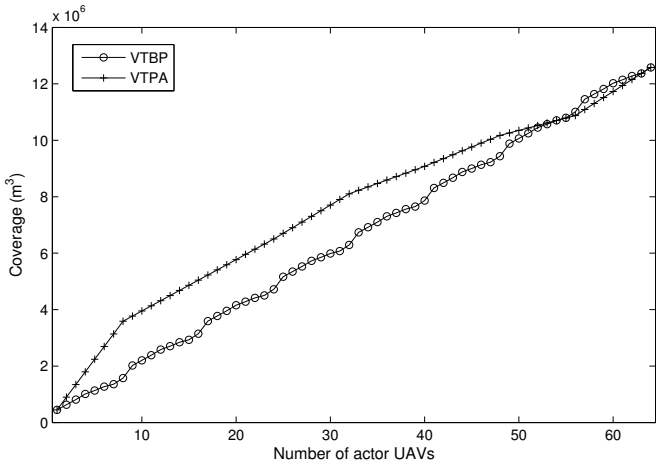

Fig. 7: 1-hop coverage for VTBP vs. VTPA.

structure. Fig. 5 and Fig. 6 show the coverage for a single sink and two sinks geometries of both methods, respectively. The coverage characteristic of our method outperforms PRB in both cases and the performance difference becomes higher as the number of actors increase.

Fig. 7 show the coverage for VSEPR theory based positioning (VTBP) and VSEPR theory based positioning with preferential attachment based actor deployment (VTPA) for increasing number of actors up to eight sinks. In this experiment, the main objective is to see the effects of balanced and preferential attachment based actor deployment in total covered volume for multiple sink geometries. The topologies with the balanced actor deployment have significantly larger coverage as the number of actors is below 50. After the number of actors exceeds 50, the performances of the approaches are very close to each other since the probability of forming different geometries decreases and the topologies become very similar.

The coverage calculations assume spherical communication ranges for UAVs with identical RSSI and loss rates at every communication angle. These factors are effective in the performance of real life UAV systems. Therefore, the antenna configuration has an important role when designing protocols for aerial networks. Depending on the number of actors and the selected VSEPR theory geometry, our approach requires communication in various directions and distances for the actors. Therefore, our positioning strategy must be combined with efficient control message exchange mechanisms and high throughput data transfer opportunities. The antenna configuration must provide neighbor discovery in 360 degrees and low-interference communication with high throughput.

UAVs can be equipped with different types of antennas such as omnidirectional and bidirectional antennas. While omnidirectional antennas enable 360 degrees of coverage when needed, the directional antennas provide high throughput and low interference. Therefore, Omni Bi-directional ESPAR (O-BESPAR) [44] antenna model would satisfy the requirements of our approach as it provides these properties by leveraging the complementary properties of omni-directional and directional antennas. The control messages can be transmitted by using the omni module of O-BESPAR since the beamforming can be steered to any direction. However, the restrictions of the omni module must also be taken into account. The omnidirectional antenna has a transmission range smaller than the directional ESPAR module and it is not completely

isotropic as its orientation affects the RSSI value [45]. If it is used for neighbor discovery in our positioning approach, the distances among the nodes must be arranged according to the observed RSSI values. The transmission power, antenna gain, distances and antenna positions are also important factors for the path loss and propagation models. The control messages transmitted by the omni module allow locating the neighbor UAVs. Then the directional modules of O-BESPAR provides simultaneous high throughput data transmission and reception after beams of two UAVs are steered to each other in the correct angles. The angles for the directional modules are calculated by using the GPS receivers and altitude sensors on the UAVs. The directional module can also be used for neighbor discovery by using bi-directional beam sweeping. This method would increase the coverage of the network while adding a scanning delay for the sweeping.

B. Weight

The weight attribute of the nodes is used as another metric for the performance evaluation of our approach. Sensor UAVs store the weight values for the actors they are affiliated with and it is equal to the "k-(hop distance)" where k is the weight of the actor and hop distance is the number of hops required to reach the affiliated actor. The weight of a sensor UAV decreases by one with each hop it gets further from the actor.

The collected information on a sensor UAV can be transmitted to an actor through the path of the sensor UAVs with increasing weight values. Therefore, in contrast to many of the 3D positioning approaches in literature, the coverage of the 3D space is not the only critical criterion to measure the performance of our approach. The sensor measurements can be collected from a large volume of space by utilizing the weight attribute of the sensor nodes. Therefore, we use another metric, average weight value, instead of coverage for the performance assessment of our protocol.

Fig. 8 shows the maximum and the minimum weight values averaged over the nodes for all possible geometries. The geometries formed by more actors result in higher average weight values in the network, which means less number of hops for the sensor nodes to transmit the collected information to the actors. The number of unconnected nodes is also decreasing as the geometries become larger. An interesting characteristic of the graph in Fig. 8 is the high difference in the average weight between trigonal planar geometry to tetrahedral geometry. Thus, it shows that the geometry gives better performance when more than one plane of actors are used.

The dynamic topology is a fundamental characteristic of our application scenario. Sensor UAVs fly continuously with perturbations in their main flight paths. While the average weight value is critical, the maximum and minimum weight values are also important to assess the suitability of our positioning approach to the mobility of the nodes in our application scenario. The maximum and the minimum hop number of the sensor nodes must not vary among actor areas in a network where the sensor nodes are shared efficiently among actors.

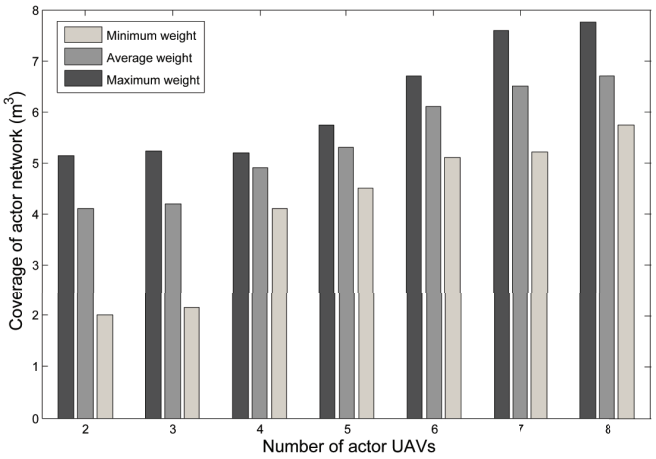

Fig. 8: Average, maximum and minimum $weight$ values for all geometries.

Fig. 8 shows that the sensor UAVs are affiliated with the actor UAVs within a smaller range of possible weight values as the number of actor UAVs increase. When the difference between the values of average minimum weight and the average weight values is high, it indicates an ineffective sharing of the nodes as they move in the network. It can be observed that as the geometries evolve, the average minimum weight value increases and the range of weight values that the nodes acquire becomes smaller. Additionally, the performance of the system improves considerably from the trigonal planar geometry to tetrahedral geometry. Therefore the results show that the performance improvement is not only affected by the increase in the number of actors but it also depends on the geometries used.

C. Cardinality

The cardinality of an actor represents the number of sensor nodes affiliated with that actor. While using multiple actors, the concurrency becomes essential for an effective utilization of the system. As a result, cardinality is chosen as the metric to evaluate the performance of the system in distributing the actor affiliations. For the experiment scenarios, sensor nodes move with random mobility in the environment.

The average cardinality of the actors are shown in Fig. 9 with the range of the collected values. The results show that the average cardinality increases as the number of actors increases. The percentage variation in the cardinalities takes values from 10% to 20% for different geometries. Low fluctuation in the observed values is a result of a balanced sharing of the sensor nodes by the actors in the network.

D. Betweenness centrality

The betweenness centrality represents a measure of positional importance of a node in the network. When a node a is in the shortest path between two other nodes, these two nodes depend on the node a for communication. The betweenness centrality for a sink in the application scenario of our approach is the sum of the fraction of all shortest path pairs passing through the sink a, defined as follows:

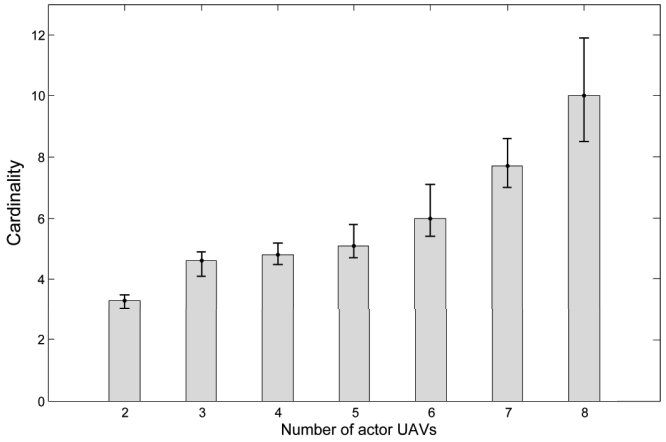

Fig. 9: Cardinality of actors for different geometries.

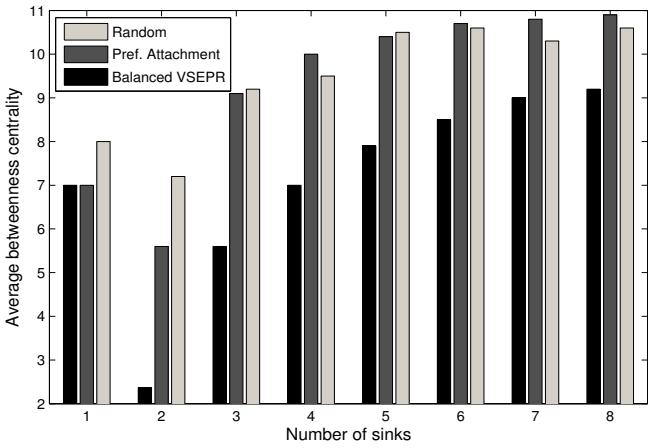

Fig. 10: Average betweenness centrality of sink nodes.

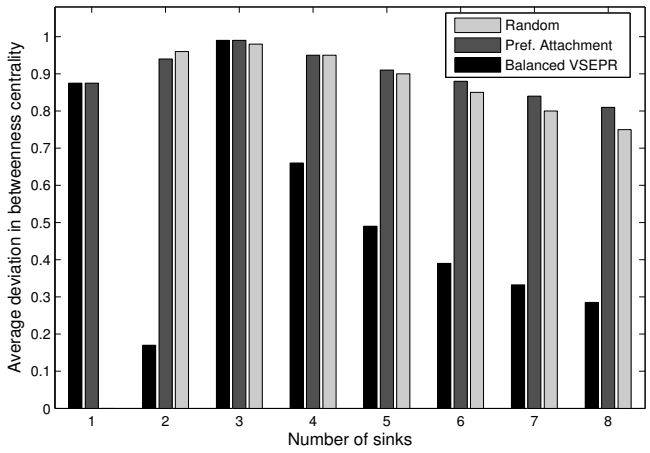

Fig. 11: Average deviation in betweenness centrality of sink nodes.

$$c_B(a) = \sum_{s,t=V} \frac{\sigma(s,t \mid a)}{\sigma(s,t)}$$

where V is the set of nodes, $\sigma(s,t)$ is the number of shortest (s,t) paths, and $\sigma(s,t \mid a)$ is the number of those paths passing through a.

VSEPR theory is the most successful approach for molecular geometry predictions. Our previous simulations show that our adoption of VSEPR theory results in high performance in coverage. However VSPER theory is not analyzed in terms of the network characteristics of the created geometries. For this analysis, we first use the betweenness centrality. Betweenness centrality values in our application scenario is more important for sinks since all of the actors are the leaves of the network.

We compare the performances for the cases, where the actors are deployed by random deployment, preferential attachment based approach and our balanced approach. Fig. 10 shows the average betweenness centrality values of the sinks for geometries with different number of sinks and Fig. 11 presents the average deviation of betweenness centrality for the sink nodes. The results given in Fig. 10 and Fig. 11 show that the preferential attachment based approach has higher values both for average betweenness centrality and the average deviation in betweenness centrality of sink nodes. Fig. 11 shows that the average deviation in betweenness centrality decreases for all methods as the number of sinks exceeds three. The value for our approach decreases to one third of its value as the number of sinks increases from three to eight whereas the change in other approaches is about 10% under the same conditions. VSEPR theory based balanced approach provides larger coverage values for all of cases. Therefore, the average deviation in betweenness centrality must be smaller for a better coverage performance in our approach.

E. Clustering coefficient

Another metric used to analyze the network characteristics of our approach is the clustering coefficient (CC). CC is used as a measure showing how concentrated the neighborhood of a node is in the network. It is also used to show the tendency of the nodes to cluster together. The network graph formed by the VSEPR topologies are unweighted and the CC of a node u in this unweighted graph is the fraction of possible triangles through that node, which is defined as follows:

$$c_u = \frac{2T(u)}{deg(u)(deg(u)-1)}$$

where $T(u)$ is the number of triangles through node u and $deg(u)$ is the degree of u.

We compare the CC values of the sinks for the geometries formed by the deployment of actors based on random deployment, preferential attachment based approach and our balanced approach.

Fig. 12 shows the average sink CC for the geometries with different number of sinks. The sink CC increases as the geometries become larger. The preferential attachment based approach has the highest and the VSEPR based balanced approach has the lowest sink CC values for all of the geometries whereas the values for random positioning are in between the other two approaches.

Fig. 13 shows the average CC values of actors for various number of sinks. For all of the cases, balanced VSEPR based approach has smaller average CC compared to preferential attachment based approach. Random positioning method has

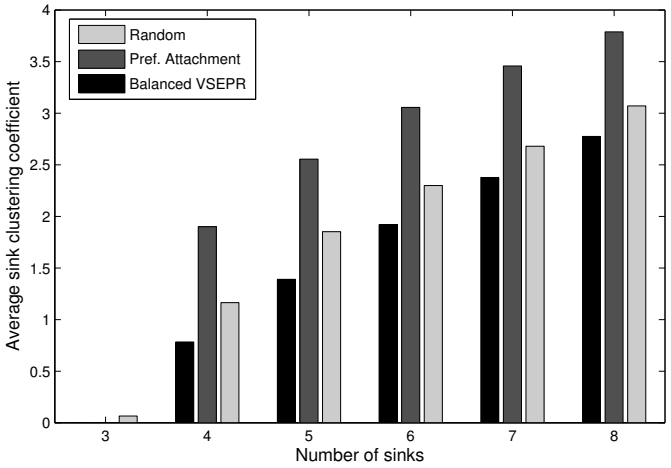

Fig. 12: Average sink clustering coefficient for different number of sinks.

values in between the other two approaches most of the time.

The results given in Fig. 12 and Fig. 13 show that the preferential attachment based approach has higher CC values both for actors and the sinks. However VSEPR theory based balanced approach has a larger coverage for all different cases. Therefore, the results indicate that the coverage of UAV network is inversely proportional to the clustering in our approach.

V. Conclusion

In this paper, we introduced a node positioning strategy for aerial networks. The goal of the approach is to improve the on-site monitoring of a 3D volume in an application scenario with multiple UAVs. The UAV network is modeled with a wireless sensor and actor network structure based on different capabilities of the node types in the network. The positioning algorithm utilizes VSEPR theory to overcome the challenges of the application scenario. The basic rules of VSEPR theory are extended to overcome the limitation on the number of actors and only local communication is required for actor positioning. The extensive simulation study shows that the system provides high coverage while keeping 1-hop connectivity between each actor and a sink. A future direction for this work would be the adoption of different molecular clustering structures for UAV applications according to their specific requirements. Another future direction would be the adaptation of the proposed approach for the environmental conditions of the monitored space, which may limit the possible geometries formed by the UAV network.

Acknowledgement

The authors would like to thank Riverbed Technology Inc. for supporting this research by providing OPNET Modeler software under University Program.

References

[1] I. Bekmezci, O. K. Sahingoz, and S. Temel, "Flying Ad-Hoc Networks (FANETs): A survey," *Ad Hoc Networks*, vol. 11, no. 3, pp. 1254–1270, May 2013.

[2] I. F. Akyildiz and I. H. Kasimoglu, "Wireless sensor and actor networks: research challenges," *Ad Hoc Networks*, vol. 2, no. 4, pp. 351–367, October 2004.

[3] S. Thrun, M. Diel, and D. Hähnel, "Scan Alignment and 3-D Surface Modeling with a Helicopter Platform," *Field and Service Robotics, Springer Tracts in Advanced Robotics*, vol. 24, pp. 287–297, 2006.

[4] G. Astuti, G. Giudice, D. Longo, C. D. Melita, G. Muscato, and A. Orlando, "An Overview of the 'Volcan Project': An UAS for Exploration of Volcanic Environments," *J. Intell. Robotic Syst.*, vol. 54, no. 1-3, pp. 471–494, March 2009.

[5] T. P. Ackerman and G. M. Stokes, "The Atmospheric Radiation Measurement Program," *Physics Today*, vol. 56, no. PNNL-SA-37894, 2003.

[6] V. Ramanathan, M. V. Ramana, G. Roberts, D. Kim, C. Corrigan, C. Chung, and D. Winker, "Warming trends in Asia amplified by brown cloud solar absorption," *Nature*, vol. 448, no. 7153, pp. 575–578, 2007.

[7] M. R. Brust and B. M. Strimbu, "A networked swarm model for UAV deployment in the assessment of forest environments," in *IEEE Conference on Intelligent Sensors, Sensor Networks and Information Processing (ISSNIP)*, 2015, pp. 1–6.

[8] R. Gillespie and R. Nyholm, "Inorganic stereochemistry," *Quart. Rev. Chem. Soc.*, vol. 11, pp. 339–380, 1957.

[9] M. İ. Akbaş and D. Turgut, "Lightweight Routing with QoS Support in Wireless Sensor and Actor Networks," in *Proceedings of the IEEE Global Telecommunications Conference (GLOBECOM)*, December 2010, pp. 1–5.

[10] S. Lee and M. Younis, "Optimized relay node placement for connecting disjoint wireless sensor networks," *Computer Networks*, vol. 56, pp. 2788–2804, Aug. 2012.

[11] M. İ. Akbaş and D. Turgut, "Lightweight routing with dynamic interests in wireless sensor and actor networks," *Ad Hoc Networks*, vol. 11, no. 8, pp. 2313–2328, 2013.

[12] V. Ravelomana, "Extremal properties of three-dimensional sensor networks with applications," *IEEE Transactions on Mobile Computing*, vol. 3, no. 3, pp. 246–257, August 2004.

[13] P. Li, M. Pan, and Y. Fang, "The Capacity of Three-Dimensional Wireless Ad Hoc Networks," in *Proceedings of the IEEE International Conference on Computer Communications (INFOCOM)*, April 2011, pp. 1485–1493.

[14] K. Akkaya and A. Newell, "Self-deployment of sensors for maximized coverage in underwater acoustic sensor networks," *Computer Communications*, vol. 32, no. 7-10, pp. 1233–1244, May 2009.

[15] N. Peppas and D. Turgut, "A hybrid routing protocol in wireless mesh networks," in *Proceedings of the IEEE Military Communications Conference (MILCOM)*, October 2007.

[16] S. N. Alam and Z. J. Haas, "Coverage and connectivity in three-dimensional networks with random node deployment," *Ad Hoc Networks*, September 2014.

[17] H. Zhou, S. Xia, M. Jin, and H. Wu, "Localized algorithm for precise boundary detection in 3D wireless networks," in *Proceedings of International Conference on Distributed Computing Systems*, June 2010, pp. 744–753.

[18] X. Bai, C. Zhang, D. Xuan, and W. Jia, "Full-coverage and k-connectivity (k =14, 6) three dimensional networks," in *Proceedings of IEEE International Conference on Computer Communications (INFOCOM)*, April 2009, pp. 388–396.

[19] P. I.-S. Chiang and W.-C. Peng, "Slab Routing: Adapting Two-Dimensional Geographic Routing to Three-Dimensions," in *Proceedings of the of IEEE International Conference on Sensing, Communication and Networking (SECON)*, July 2009, pp. 1–9.

[20] K.-P. Lin and K.-C. Hung, "An efficient fuzzy weighted average algorithm for the military UAV selecting under group decision-making," *Elsevier Knowledge-Based Systems*, vol. 24, no. 6, pp. 877–889, August 2011.

[21] M. Israel, "A UAV-based roe deer fawn detection system," *International Archives of the Photogrammetry, Remote Sensing and Spatial Information Sciences (ISPRS)*, vol. 38-1/C22, pp. 51–55, September 2011.

[22] G. Tuna, T. V. Mumcu, K. Gulez, V. C. Gungor, and H. Erturk, "Unmanned aerial vehicle-aided wireless sensor network deployment system for post-disaster monitoring," in *Emerging Intelligent Computing Technology and Applications*. Springer, 2012, pp. 298–305.

[23] H. Chao, Y. Cao, and Y. Chen, "Autopilots for small fixed-wing unmanned air vehicles: A survey," in *Proceedings of the IEEE International Conference on Mechatronics and Automation (ICMA)*, August 2007, pp. 3144–3149.

[24] M. E. Dempsey, "Eyes of the army–US Army roadmap for unmanned aircraft systems 2010–2035," *US Army UAS Center of Excellence, Ft. Rucker, Alabama*, vol. 9, 2010.

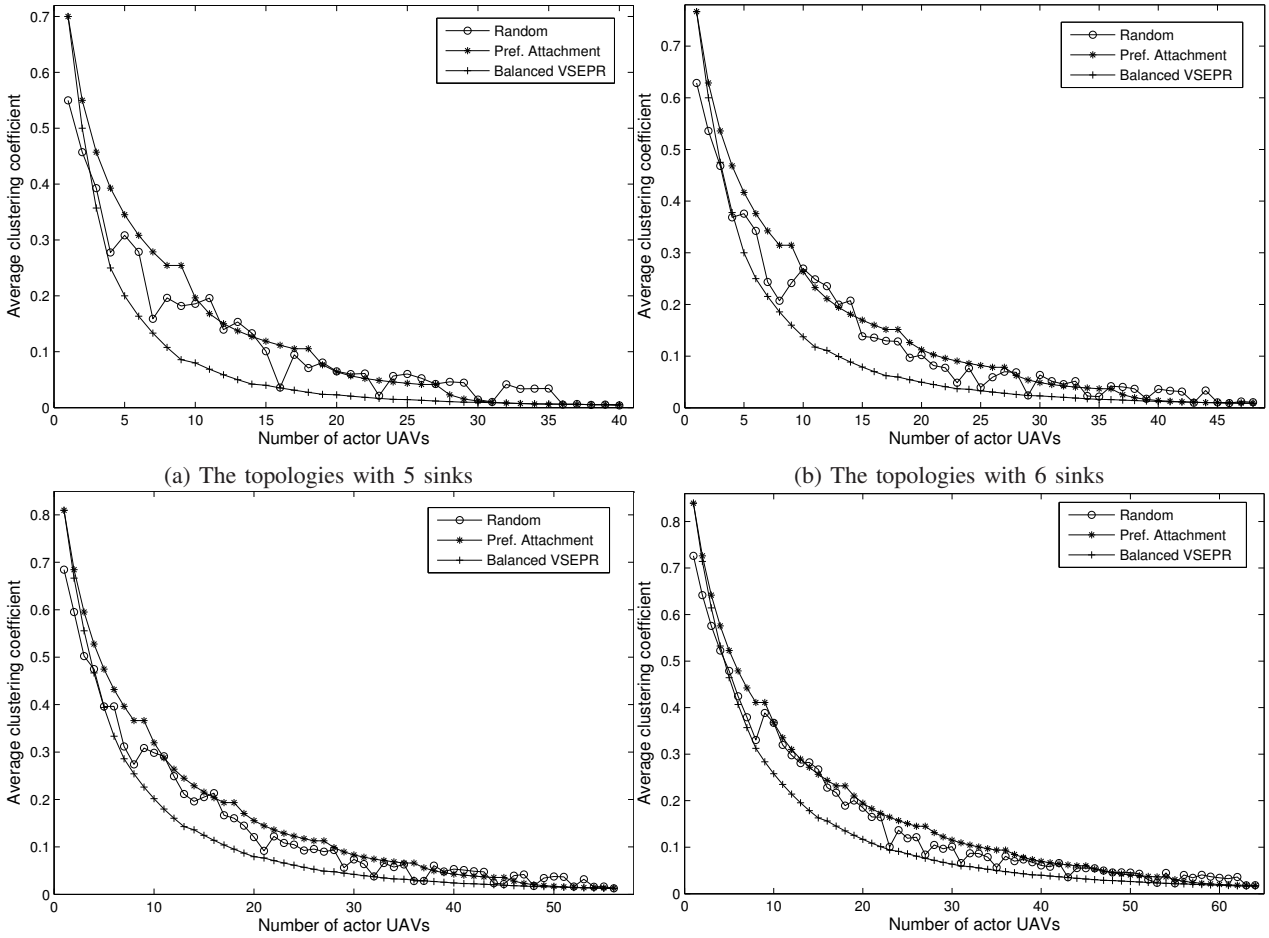

(a) The topologies with 5 sinks

(b) The topologies with 6 sinks

(c) The topologies with 7 sinks

(d) The topologies with 8 sinks

Fig. 13: Average clustering coefficient values of actors for different number of sinks.

[25] A. Brecher, V. Noronha, and M. Herold, "A roadmap for deploying unmanned aerial vehicles (UAVs) in transportation," in *US DOT/RSPA: Volpe Center and NCRST Infrastructure, Specialist Workshop*, December 2003.

[26] P. Li, C. Zhang, and Y. Fang, "The capacity of wireless ad hoc networks using directional antennas," *IEEE Transactions on Mobile Computing*, vol. 10, no. 10, pp. 1374–1387, Oct. 2011.

[27] J. Jiang, C. Lin, and Y. Hsu, "Localization with rotatable directional antennas for wireless sensor networks," in *Proceedings of the International Conference on Parallel Processing Workshops (ICPPW)*. IEEE, 2010, pp. 542–548.

[28] A. Alshbatat and L. Dong, "Performance analysis of mobile ad hoc unmanned aerial vehicle communication networks with directional antennas," *International Journal of Aerospace Engineering*, vol. 2010, 2011.

[29] S. Temel and I. Bekmezci, "LODMAC: Location Oriented Directional MAC protocol for FANETs," *Computer Networks*, vol. 83, pp. 76–84, Jun. 2015.

[30] Z. Zhang, "Performance of neighbor discovery algorithms in mobile ad hoc self-configuring networks with directional antennas," in *Proceedings of the IEEE Military Communications Conference (MILCOM)*, Oct. 2005, pp. 3162–3168.

[31] A. Purohit and P. Zhang, "Sensorfly: A controlled-mobile aerial sensor network," in *Proceedings of the ACM Conference on Embedded Networked Sensor Systems (SenSys)*, November 2009, pp. 327–328.

[32] J. Elston and E. Frew, "Hierarchical Distributed Control for Search and Tracking by Heterogeneous Aerial Robot Networks," in *Proceedings of the IEEE International Conference on Robotics and Automation (ICRA)*, May 2008, pp. 170–175.

[33] M. Dumiak, "Robocopters Unite!" *IEEE Spectrum*, vol. 46, no. 2, p. 12, February 2009.

[34] J. Allred, A. B. Hasan, S. Panichsakul, W. Pisano, P. Gray, J. Huang, R. Han, D. Lawrence, and K. Mohseni, "SensorFlock: An airborne wireless sensor network of micro-air vehicles," in *Proceedings of the ACM Conference on Embedded Networked Sensor Systems (SenSys)*, November 2007, pp. 117–129.

[35] C. Luo, S. McClean, G. Parr, L. Teacy, and R. De Nardi, "UAV Position Estimation and Collision Avoidance Using the Extended Kalman Filter," *IEEE Transactions on Vehicular Technology*, vol. 62, no. 6, pp. 2749–2762, 2013.

[36] L. A. Villas, A. Boukerche, D. L. Guidoni, G. Maia, and A. A. F. Loureiro, "A Joint 3D Localization and Synchronization Solution for Wireless Sensor Networks Using UAV," in *Proceedings of the IEEE International Conference on Local Computer Networks (LCN)*, October 2013, pp. 736–739.

[37] G. Lee, Y. Nishimura, K. Tatara, and N. Y. Chong, "Three dimensional deployment of robot swarms," in *Proceedings of the IEEE/RSJ International Conference on Intelligent Robots and Systems (IROS)*, October 2010, pp. 5073–5078.

[38] N. V. Sidgwick and H. M. Powell, "Bakerian Lecture. Stereochemical Types and Valency Groups," *Proceedings of the Royal Society A*, vol. 176, no. 965, pp. 153–180, October 1940.

[39] R. J. Gillespie, "The electron-pair repulsion model for molecular geometry," *Journal of Chemical Education*, vol. 47, no. 1, p. 18, January 1970.

[40] M. İ. Akbaş and D. Turgut, "APAWSAN: Actor positioning for aerial wireless sensor and actor networks," in *Proceedings of the IEEE Conference on Local Computer Networks (LCN)*, October 2011, pp. 567–574.

[41] S. F. A. Kettle, *Theoretical Chemistry Accounts*, vol. 3, no. 2, p. 211, 1965.

[42] J. Clapper, J. Young, J. Cartwright, and J. Grimes, "Unmanned Systems Roadmap 2007-2032," Dept. of Defense, Tech. Rep., 2007.

[43] "OPNET Modeler," http://www.opnet.com.

[44] K. Li, N. Ahmed, S. S. Kanhere, and S. Jha, "Reliable communications in aerial sensor networks by using a hybrid antenna," in *Proceedings of the IEEE International Conference on Local Computer Networks (LCN)*. IEEE, October 2012, pp. 156–159.

[45] N. Ahmed, S. S. Kanhere, and S. Jha, "Link Characterization for Aerial Wireless Sensor Networks," in *Proceedings of the IEEE Global Telecommunications Conference (GLOBECOM) Workshops*, December 2011, pp. 1274–1279.